

Influence of Pedaling Rate on Muscle Mechanical Energy in Low Power Recumbent Pedaling Using Forward Dynamic Simulations

Nils A. Hakansson and M. L. Hull

Abstract—An understanding of the muscle power contributions to the crank and limb segments in recumbent pedaling would be useful in the development of rehabilitative pedaling exercises. The objectives of this work were to 1) quantify the power contributions of the muscles to driving the crank and limb segments using a forward dynamic simulation of low-power pedaling in the recumbent position, and 2) determine whether there were differences in the muscle power contributions at three different pedaling rates. A forward dynamic model was used to determine the individual muscle excitation amplitude and timing to drive simulations that best replicated experimental kinematics and kinetics of recumbent pedaling. The segment kinematics, pedal reaction forces, and electromyograms (EMG) of 10 muscles of the right leg were recorded from 16 subjects as they pedaled a recumbent ergometer at 40, 50, and 60 rpm and a constant 50 W workrate. Intersegmental joint moments were computed using inverse dynamics and the muscle excitation onset and offset timing were determined from the EMG data. All quantities were averaged across ten cycles for each subject and averaged across subjects. The model-generated kinematic and kinetic quantities tracked almost always within 1 standard deviation (SD) of the experimental data for all three pedaling rates. The uniaxial hip and knee extensors generated 65% of the total mechanical work in recumbent pedaling. The triceps surae muscles transferred power from the limb segments to the crank and the bi-articular muscles that crossed the hip and knee delivered power to the crank during the leg transitions between flexion and extension. The functions of the individual muscles did not change with pedaling rate, but the mechanical energy generated by the knee extensors and hip flexors decreased as pedaling rate increased. By varying the pedaling rate, it is possible to manipulate the individual muscle power contributions to the crank and limb segments in recumbent pedaling and thereby design rehabilitative pedaling exercises to meet specific objectives.

Index Terms—Adaptive muscle control, biological motor systems, muscle power, pedaling exercise, rehabilitation.

I. INTRODUCTION

RECURBENT pedaling is a therapeutic activity that provides benefit for a broad range of medical conditions requiring rehabilitation. Recumbent ergometers have large seats with seatbacks to provide support for the upper body, and are low to the ground, permitting easy access for individuals with

mobility impairments. Recumbent pedaling has been demonstrated to be a therapeutic modality for exercise and rehabilitation for individuals following a stroke [1], peripheral neuropathy [2], and spinal cord injury [1], [3]–[5].

Because recumbent pedaling is used as a therapeutic exercise, it is of interest to investigate muscle kinetics (i.e., force, work, and power) in recumbent pedaling. Understanding muscle kinetics is important because they are the mechanical demands on the individual muscle and tendon structures which are responsible for movement. Therefore, an investigation of muscle kinetics could provide information that would be useful in the design of rehabilitation protocols to improve the effectiveness of existing pedaling therapies and develop new pedaling therapies for the diseased and disabled population. For example, the determination of individual muscle powers and their influence on the limb segments in recumbent pedaling could have implications for improved pedaling therapies to address issues such as anterior cruciate ligament (ACL) rehabilitation [6] and patellofemoral pain [7].

Though several studies on individual muscle kinetics during pedaling have been performed, the applicability of these studies to a rehabilitative setting is limited. Previous work utilizing forward dynamic simulations, which provide the means to determine individual muscle powers and their respective contributions to driving the crank and the limb segments [8]–[10], has determined muscle kinetics for relatively high-workrate upright pedaling [9], [11]–[13] and for recumbent pedaling when the muscles have been excited by means of external electrical stimulation [14]–[16]. The workrates used in the upright pedaling studies reflect those of competitive and elite cyclists and are well above those that would be used in a rehabilitative setting. Whereas the recumbent pedaling simulations were conducted to achieve rehabilitative goals, the muscles in these studies were driven by external electrical stimulation. As a result, the recumbent studies were directed at developing rehabilitative pedaling exercises for individuals with spinal cord injury and would not be applicable to individuals who activate their muscles volitionally. Because a mechanical energy analysis of recumbent pedaling using variables relevant to rehabilitation of individuals with volitional muscle control has not been performed, one objective of this study was to examine and quantify the power contributions of each muscle to driving the crank and limb segments at a workrate and pedaling rate representative of the rehabilitation setting.

Pedaling rate is an important yet not fully understood aspect of pedaling. Previous research has shown that the preferred pedaling rate is not the most efficient (e.g., [17]–[20]). Other research has demonstrated that pedaling rate influences the onset

Manuscript received April 11, 2006; revised February 5, 2007; accepted May 23, 2007. This work was supported by the National Institute for Disability and Rehabilitation Research (NIDRR) under Award H133G0200137.

Nils A. Hakansson is with the Biomedical Engineering Program, University of California, Davis, CA 95616 USA (e-mail: nahakansson@ucdavis.edu).

M. L. Hull is with the Department of Mechanical Engineering and the Biomedical Engineering Program, University of California, Davis, CA 95616 USA (e-mail: mlhull@ucdavis.edu).

Digital Object Identifier 10.1109/TNSRE.2007.906959

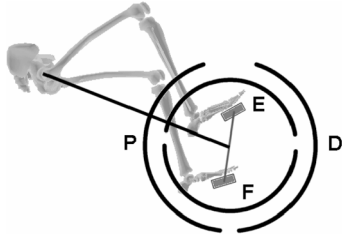


Fig. 1. Position of the seat in the recumbent position relative to the crank spindle. Beginning of the crank cycle (0°) was defined when the right crank arm was directed toward the hip center. Also illustrated are the four primary regions of the crank cycle for recumbent pedaling from Hakansson and Hull (2005). Four regions indicated are the extension (E), distal transition (D), flexion (F), and proximal transition (P) region.

and offset timing of individual muscles in pedaling [19], [21], [22]. However, the effect of pedaling rate on individual muscle power contributions to driving the crank and limb segments has not been investigated. The understanding gained from an analysis of the muscle mechanical energy and pedaling rate relationship could result in more effective exercise and rehabilitation strategies for conditions such as patellofemoral pain, ACL reconstruction, and peripheral neuropathy. Therefore, the second objective of this study was to examine the effect of different pedaling rates representative of the rehabilitation setting on the muscle power contributions required to simulate recumbent pedaling.

II. METHODS

A. Model Development and Simulation

The planar two-legged model developed by Neptune and Hull [23] with SIMM (MusculoGraphics, Inc., Santa Rosa, CA) formed the basis of the bicycle-rider model used in our recumbent pedaling simulations. In summary, each leg was modeled as three segments (thigh, shank, and foot) with the foot rigidly attached to the pedal. The two pedals were connected to a crank that rotated about an axis fixed in the inertial frame. All joints were modeled as revolute except for the knee, which was modeled as a single degree-of-freedom planar joint with two translational degrees-of-freedom that were constrained by the knee flexion angle [24]. The patella was constrained to follow a set path relative to the femur and defined as a function of knee flexion angle [25]. Each leg was treated as symmetric but 180° out of phase with the contralateral limb. A torque equivalent to the resistive and inertial torque produced by the ergometer was applied about the rotational axis of the crankarm in the model [26]. The effective inertia of the ergometer crank (e.g., the pedals, crank arms, chain rings, and flywheel) was computed using the manufacturer specifications of the flywheel and components [26] and verified with measurements of spin-down time of the unoccupied ergometer at different levels of braking friction [14]. The fixed axis of the crank was positioned relative to the pelvis to account for the recumbent pedaling position (Fig. 1).

The muscle contraction dynamics were based on a generic Hill-type lumped-parameter model [27]. The muscle origin and insertion points and the muscle moment arm lengths, calculated from origin and insertion points and joint angle, were from the work of Delp *et al.* [25]. Via points along the musculo-tendon

path designated by Delp *et al.* [25] for cases in which the muscle either wraps around bone or is constrained by retinacula were also used.

A forward dynamic model was generated using Dynamics Pipeline (MusculoGraphics, Inc., Santa Rosa, CA, USA) from the equations of motion for the rider-ergometer system derived using SD/FAST (Parametric Technology Corp., Needham, MA, USA). Fourteen muscles per leg grouped into nine muscle sets were used to drive the model. The 14 muscles were grouped into functional muscle sets based on previous studies [9], [10], [22], [23]. The muscle groups and associated muscles were SOL (soleus), GAS (medial and lateral gastrocnemius), TA (tibialis anterior), HAM (medial hamstrings, biceps femoris long head), BFsh (biceps femoris short head), VAS (3-component vastus), RF (rectus femoris), PSOAS (iliacus, psoas), and GMAX (gluteus maximus, adductor magnus). The VAS muscle set was comprised of three pseudo-muscle components that model the knee extensor joint torque capacity of the three vasti muscles [14].

All of the muscles in a set received the same excitation signal, and the muscle excitation signals for the corresponding muscles in the contralateral limb were the same but 180° out of phase. The excitation waveform to each of the muscles was represented by a quadratic sloped pattern that defined the onset and offset angle and amplitude of the muscle excitation [28]. The activation dynamics were represented by a first-order differential equation that reflects the physiological processes to activate and deactivate the muscle [9].

The forward dynamic model was used to compute the neuromuscular excitation patterns for the muscle sets of the right and left legs that provided the best fit to the measured kinetic and kinematic data averaged across the subjects (i.e., solution to the “tracking” problem). This performance criterion minimized the difference between the experimental and simulated right horizontal and vertical pedal forces, right ankle, knee, and hip intersegmental moments, right pedal angle, and the crank torque. Tracking was performed by minimizing

$$J_{\text{RMSE}} = \sqrt{\frac{\sum_{j=1}^m \sum_{i=1}^n \frac{(Y_{ij} - \hat{Y}_{ij})^2}{\text{SD}_{ij}^2}}{mn}} \quad (1)$$

where Y_{ij} is the experimental data, \hat{Y}_{ij} is the model-generated data, n is the number of data points, m is the number of tracking quantities, and SD_{ij} is the intersubject standard deviation. The sum of the squared error term was normalized to the number of data points n to allow comparison across pedaling rates. The intersubject standard deviation weighted the tracking variables. Tracking variables with less intersubject variability were weighted more than those with greater intersubject variability.

The optimal solution to the tracking problem was obtained by converting the optimal control problem into a parameter optimization problem [29] and using a simulated annealing optimization algorithm [30] to compute the excitation parameters that minimized the cost, J_{RMSE} , and satisfied a time constraint requiring an average pedaling rate within 2 rpm of the target. The performance criterion (1) and time constraint were evaluated on the fourth cycle of the simulation to enable the simulation to reach steady state and become independent of the initial

conditions [23]. To ensure a physiologically viable result, the solution space for the muscle excitation onset and offset timing was limited to be within 2 SDs of the mean experimental electromyographic (EMG) onset and offset data.

The results of the forward simulations were used to perform a muscle power analysis to determine the muscular and nonmuscular power components to drive the crank and limbs in recumbent pedaling [8]. Individual muscle power contributions to satisfy the pedaling mechanics were determined by a segment power analysis [8]–[10]. To perform the power analysis, the individual segments were grouped together as limbs (ipsilateral thigh, shank, and foot) and crank (pedals, crank arms, chain rings, and flywheel) [8]. The net mechanical energy generated by an individual muscle over a crank cycle was calculated by integrating the instantaneous muscle power over the crank cycle. The mechanical energy flow relationships and the linear transformation between segment acceleration and power [8] were used to interpret how the muscle's power contributed to the power of the limb segments and crank. The crank cycle was divided into four regions (i.e., extension (E), distal transition (D), flexion (F), and proximal transition (P) region) [22] (Fig. 1) to assist in the analysis of the muscle power contribution to pedaling.

B. Experiments

Experimental data was collected from subjects to provide data for the tracking problem. Written informed consent was obtained from sixteen active cyclists (fifteen male, one female) who volunteered for the study. The age of the subjects ranged from 18 to 60 years (mean 30.0 ± 11.6 years), the heights ranged from 1.63 to 1.91 m (mean 1.80 ± 0.07 m), and the weights ranged from 59 to 82 kg (mean 71.0 ± 6.0 kg). None of the subjects rode a recumbent ergometer on a regular basis. The experimental protocol was approved by the Institutional Review Board of the University of California at Davis.

Kinematic, kinetic, and EMG data were collected from the subjects as they pedaled a recumbent ergometer (Scifit ISO1000R, Tulsa, OK) that allowed a constant workrate to be set independent of pedaling rate. To prevent potential hyper-extension of the knee, the seat position was set relative to the crank spindle such that the subjects' knee angle with the ankle in the neutral position was flexed at least 45° (full extension equals 0°) at any point in the crank cycle [31]. The subjects all used zero-float clipless pedals (i.e., cleats) and chose their own cleat angle. Ergometer crank angle data and subject limb kinematics were determined using high-resolution video-based motion analysis (Motion Analysis Corp., Santa Rosa, CA). Two spherical reflective markers were placed 30 cm apart in line with the top surface of the pedal and three spherical markers were placed at three fixed points on the ergometer. These two sets of markers were used to develop virtual markers to identify the pedal and crank spindles [22]. The right crank arm directed toward the hip center defined the beginning of the crank cycle (0° of a 360° cycle) (Fig. 1). Spherical markers were also placed over the anterior superior iliac spine (ASIS), greater trochanter, lateral epicondyle, and lateral malleolus of the right leg of each subject to capture the limb kinematics. Four high-speed video cameras recorded the 3-D marker positions. The three-dimensional marker positions were then projected on

the sagittal plane as defined by the path of the pedal spindle. The position of the hip joint center was treated as fixed and determined relative to the ASIS coordinates based on the methods developed by Neptune and Hull [32]. The external loads at the right pedal were measured using a two-load component pedal dynamometer [33]. The experimental kinematic and kinetic data recorded as the subjects pedaled the ergometer were used in conjunction with SIMM (MusculoGraphics, Inc., Santa Rosa, CA) models to compute the intersegmental moments using a standard inverse dynamics approach. Individual models scaled to each subject were generated using SIMM to ensure similar knee kinematics and thereby reduce inconsistencies between the inverse and forward solutions.

EMG data collection and processing to determine the muscle excitation onset and offset were similar to that performed previously [22]. Briefly, surface EMG electrodes were placed over the belly of the soleus, medial gastrocnemius, lateral gastrocnemius, tibialis anterior, vastus medialis, vastus lateralis, rectus femoris, biceps femoris, medial hamstring, and the gluteus maximus of the right leg to examine muscle activity. The pre-amplified surface electrodes (Motion Lab Systems, Baton Rouge, LA Model MA-300-10) were fit with custom-made silver-silver chloride electrode cups (In Vivo Metric, Healdsburg, CA) and placed according to the recommendations of Delagi *et al.* [34]. The electrode cups were filled with electrode cream and the electrodes were attached to the shaved, abraded skin surface with adhesive washers. Following placement, an adhesive elastic wrap was wrapped around the leg to secure the electrode attachments.

The subjects pedaled at 90 rpm with a workrate of 125 W for 15 min to warm-up, and thereby account for temperature dependencies of muscle function [35]. The subjects then pedaled at 40, 50, and 60 rpm and a constant workrate of 50 W, which reflects the range of pedaling rates and workrates employed in studies on ergometer pedaling as a rehabilitative tool [1], [31], [36]–[38]. The pedaling rate was regulated by a metronome. The subjects pedaled at each pedaling rate for 5 min. Data were collected ten times for 4 s randomly selected intervals during the last 2 1/2 minutes of the 5-min test period. The pedaling rates were assigned randomly to control for possible interactions and fatigue.

All the data were collected and synchronized by the motion capture system. Video data were sampled at 120 Hz and filtered using a zero phase shift Butterworth low-pass filter with a cutoff frequency at 10 Hz. The pedal dynamometer and EMG signals were sampled at 1200 Hz. To reduce low frequency motion artifacts and high frequency noise, the EMG data were passed through a band-pass analog filter with low-pass cutoff of 500 Hz and high-pass cutoff of 40 Hz (manufacturer's recommendation). The 12-bit A/D board contained in the motion analysis system digitized the analog inputs. At the end of the pedaling trials, resting baseline EMG values were collected for 10 s while the subject rested in a supine position. The mean values of the rectified baseline data were used to subtract baseline offset in the EMG records. EMG burst onset and offset crank angles were determined with reference to the resting baseline data. A custom automated waveform-processing program (Matlab, The Mathworks, Natick, MA) was used to identify the burst onset and offset angles. The criteria for the burst onset and offset angles were a minimum threshold of 3 SDs of the resting baseline data

within a 50 ms moving rectangular window and a minimum 50 ms burst duration [9], [21], [22], [39]. The results for each cycle were examined graphically and the threshold was adjusted when necessary to identify the burst onset and offset angles [9], [21], [22]. The experimental EMG timing data for the muscles comprising the GAS, HAMS, and VAS muscle groups were averaged for comparison to the simulation timing data for the respective muscle group.

All of the dependent variables were computed as a function of crank angle on a cycle-by-cycle basis and averaged across cycles for each subject and then across subjects. Data were analyzed for one whole crank cycle during the 4-s intervals. Thus, the number of cycles included in the subject averages was 10.

III. RESULTS

The simulated pedaling kinetic, kinematic, and muscle excitation data tracked the averaged data from the experimental subjects well. All seven of the tracked quantities except two (the hip and ankle intersegmental moments) were within 1 SD of the experimental data; the hip and ankle intersegmental moments were almost always within 1 SD (Fig. 2). The simulated muscle excitation timing was also representative of the averaged experimental EMG timing data (Fig. 3). The average pedaling rate for the simulation at 50 rpm and 50 W was 48 rpm.

The results of the muscle power analysis for the 50 rpm and 50 W simulation indicate that the VAS and GMAX muscle groups generated the greatest peak muscle power at 46.1 W and 40.7 W, respectively (Fig. 4). Together they generated 65% (19.6 J) of the net mechanical work of the right leg (30.1 J) (Table I). The VAS muscles generated mechanical power to both the crank and limb segments, but primarily to the crank, in the extension region of the crank cycle whereas GMAX generated power primarily to the limb segments in the extension region (Fig. 4). The triceps surae muscles, SOL and GAS, transferred power from the limb segments to the crank in the extension region and then from the crank to the limb segments in the flexion region. The TA transferred power from the limb segments to the crank in the flexion region of the crank cycle. The BFsh and PSOAS muscles both absorbed power in the extension region and generated power in the flexion region of the crank cycle. BFsh absorbed power from and generated power to the crank, whereas PSOAS absorbed power from and generated power to the limb segments. Together they accounted for 41% of the net mechanical work. RF and HAM generated peak power in the proximal and distal transition regions, respectively. RF generated mechanical power to the crank in the proximal transition region of the crank cycle. HAM generated mechanical power to the crank in the distal transition region (Fig. 4).

The simulated pedaling kinetic, kinematic, and muscle excitation data from the forward dynamic models for recumbent pedaling at pedaling rates of 40 and 60 rpm and at a workrate of 50 W also tracked the respective averaged experimental data well. The average pedaling rates for the 40 and 60 rpm simulations were 38 and 58 rpm, respectively. For the 40 rpm pedaling rate model, all seven of the tracked quantities were always within 1 SD of the experimental data over the crank cycle. All of the seven quantities for the 60 rpm model except one (hip intersegmental moment) were always within 1 SD of the exper-

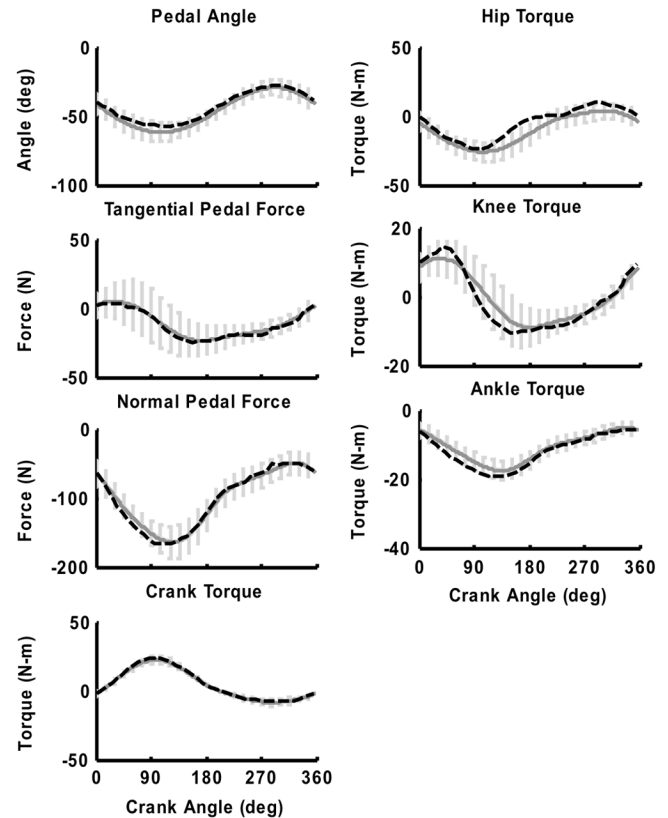


Fig. 2. Tracked kinematic and kinetic quantities from the forward simulation at 50 rpm and 50 W workrate (dashed line). Error bars represent 1 SD of the averaged experimental data. Pedal forces are represented in the pedal coordinate system with positive tangential forces directed forward and positive normal forces directed upward. For the hip and knee intersegmental moments, flexion is positive and extension is negative. For the ankle, a dorsiflexor moment is positive and plantar flexor moment is negative.

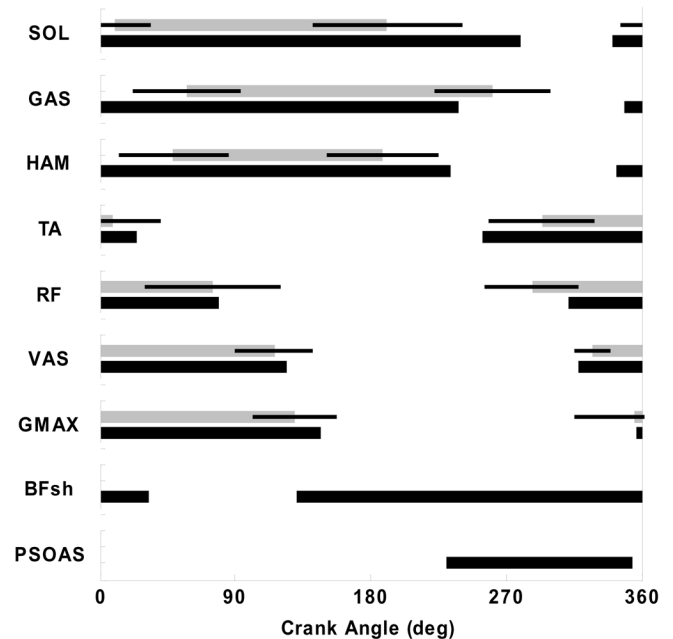


Fig. 3. Muscle excitation timing averaged across the subjects (light bars) and from the simulation (dark bars) of pedaling at 50 rpm and 50 W workrate. EMG data for the BFsh and PSOAS were not recorded from the subjects. Error bars for the averaged subject data denote ± 1 SD.

imental data; the hip intersegmental moment was within 1 SD of the experimental data for 83% of the crank cycle.

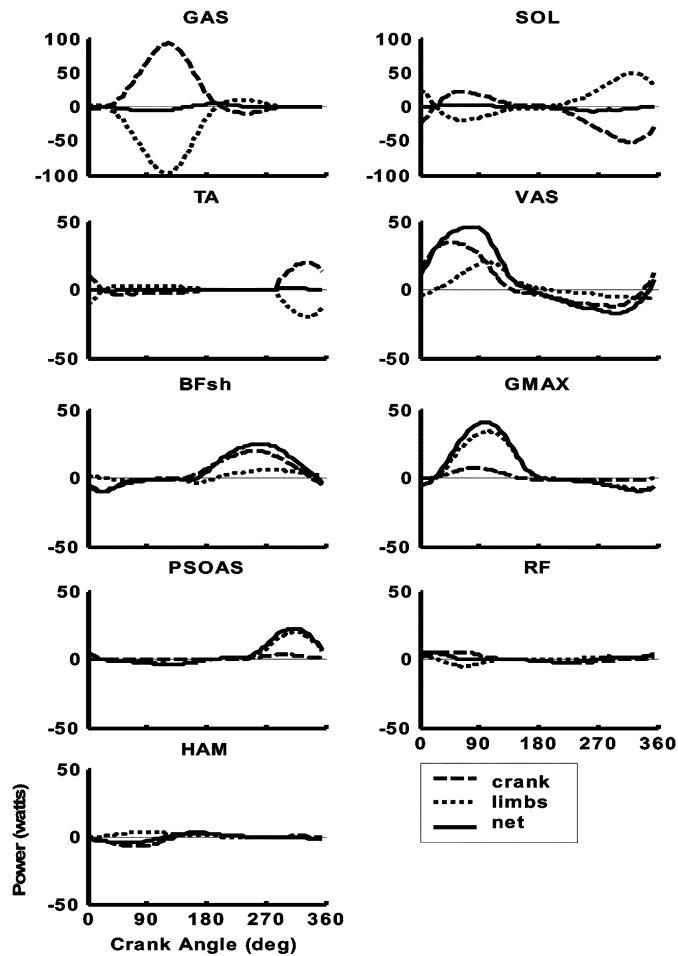


Fig. 4. Mechanical power produced by each muscle of the right leg while pedaling at 50 rpm and 50 W. Positive power indicates that energy is delivered and negative power indicates that energy is absorbed. Note the y axis scale for the GAS and SOL plots (± 100 W) is twice that of the other muscle plots (± 50 W).

The muscle power contributions at 40 and 60 rpm were similar to those for 50 rpm with a few exceptions. The net mechanical work by three of the four primary power producing muscles (VAS, BFsh, and PSOAS) decreased with increased pedaling rate (Table I). The net mechanical work contributed by GMAX, however, increased as pedaling rate increased (6.6 J at 40 rpm, 9.5 J at 50 rpm and 9.7 J at 60 rpm) (Table I). Of the remaining five muscles, two (RF and HAMS) demonstrated a trend between mechanical work and pedaling rate similar to that of VAS, BFsh, and PSOAS. No clear trend was observed for the three muscles of the lower leg (SOL, GAS, or TA) (Table I). The power profiles for the VAS and GMAX exhibited trends similar to those observed for the net mechanical work. The power profiles decreased with increased pedaling rate for the VAS and increased with increased pedaling rate for the GMAX (Fig. 5).

IV. DISCUSSION

Because recumbent pedaling is an exercise well-suited for and widely used in rehabilitation applications and because a forward dynamic model of lower power pedaling has not been created to investigate volitional muscle coordination in recumbent pedaling, the objectives of this study were 1) to quantify the work contributions of each muscle to driving the crank and limb segments at a workrate and pedaling rate representative of the re-

TABLE I
SUMMARY OF THE RESULTS FROM THE MECHANICAL ENERGY ANALYSIS FOR THE RIGHT LEG MUSCLES OVER ONE CRANK CYCLE WHILE PEDALING AT NOMINAL RATES OF 40, 50, AND 60 RPM AND A 50 W WORKRATE

Muscle	Nominal Pedaling Rate*	Pos. Mech. Energy (J)	Neg. Mech. Energy (J)	Net Mech. Energy (J)	Percent Net Mech. Energy
GAS	40 rpm	0.5	-0.8	-0.3	-0.7
	50 rpm	1.0	-1.5	-0.6	-1.9
	60 rpm	0.9	-0.5	0.4	1.4
SOL	40 rpm	2.3	-2.2	0.0	0.1
	50 rpm	1.0	-1.8	-0.8	-2.5
	60 rpm	2.4	-1.5	1.0	3.6
TA	40 rpm	0.6	-0.5	0.1	0.3
	50 rpm	0.2	-0.2	0.0	-0.2
	60 rpm	0.3	-0.2	0.1	0.4
VAS	40 rpm	20.4	-6.2	14.2	38.4
	50 rpm	16.6	-6.5	10.1	33.5
	60 rpm	12.6	-6.7	5.9	22.3
BFsh	40 rpm	10.4	-1.6	8.8	23.7
	50 rpm	9.6	-2.2	7.5	24.8
	60 rpm	9.0	-2.3	6.7	25.3
GMAX	40 rpm	9.9	-3.3	6.6	17.9
	50 rpm	12.5	-3.0	9.5	31.4
	60 rpm	13.4	-3.7	9.7	36.6
PSOAS	40 rpm	8.4	-1.5	7.0	18.9
	50 rpm	6.1	-1.2	4.9	16.2
	60 rpm	5.5	-3.0	2.5	9.4
RF	40 rpm	2.5	-0.6	1.9	5.1
	50 rpm	1.2	-0.6	0.6	2.1
	60 rpm	1.0	-0.6	0.4	1.7
HAMS	40 rpm	1.8	-3.2	-1.4	-3.7
	50 rpm	0.6	-1.6	-1.0	-3.3
	60 rpm	0.8	-1.0	-0.2	-0.7
Total	40 rpm	56.8	-19.8	37.0	100.0
All	50 rpm	48.8	-18.7	30.1	100.0
Muscles†	60 rpm	46.0	-19.5	26.5	100.0

*Actual pedaling rates in the simulations were 38, 48, and 58 rpm.

†Note that the equivalent workrate cannot be computed accurately from the pedaling rate and total muscle mechanical energy data because the pedaling rate was not constant through the crank cycle.

habilitation setting, and 2) to determine how different pedaling rates affect the muscle power contributions required to simulate recumbent pedaling. From these objectives, one key finding was that the relative mechanical energy contributions of three of the four primary power producing muscles, the VAS, GMAX, and PSOAS muscles, changed with pedaling rate whereas that of the fourth, the BFsh, did not. A second key finding was that the net mechanical energy contributions of three of the four primary power producing muscles, the VAS, PSOAS, and BFsh, decreased with increased pedaling rate, whereas that of the fourth, the GMAX, increased with increased pedaling rate.

Before addressing the importance of our findings, a discussion of the validity of the results is warranted. Because the muscle excitation timing was not tracked in the forward dynamic simulations, a comparison of the onset and offset of the simulated muscle excitation timing to the experimental timing provides a form of validation for the model results. The muscle excitation timing for the three optimal simulations was consistent with the experimental EMG data and was not at the bounds of the solution space. Accordingly, this indicates that the results of the model reproduce low power recumbent pedaling. In addition, that the simulation data followed similar trajectories as the experimental data and tracked the experimental data

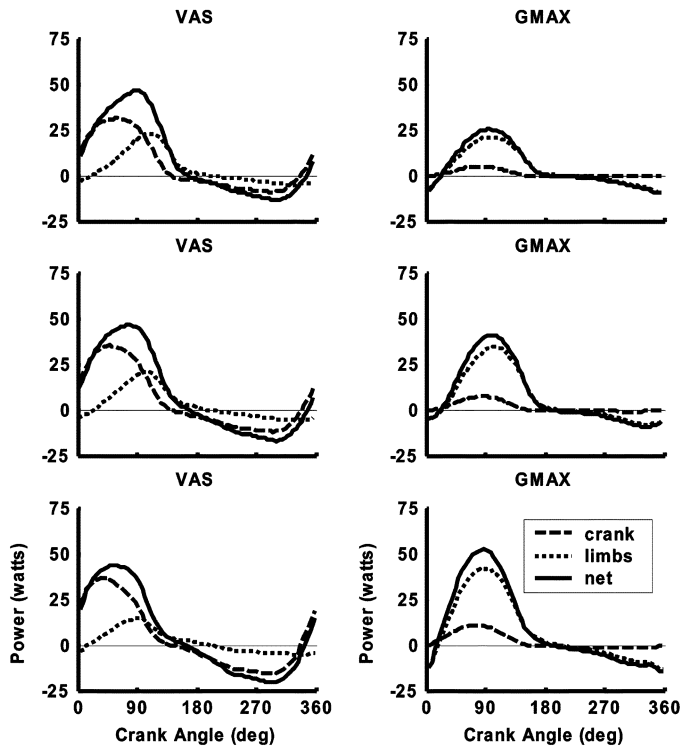


Fig. 5. Mechanical power produced by the VAS and GMAX muscle sets of the right leg while pedaling at 40 (top plots), 50 (middle plots) and 60 rpm (bottom plots) and 50 W. Plots for the 50 rpm pedaling rate are the same as in Fig. 4 and are repeated here with a different scale for comparison with the plots for the 40 and 60 rpm pedaling rates. Similar to Fig. 4, positive power indicates that energy is delivered and negative power indicates that energy is absorbed.

within 1 SD over most of the crank cycle for all but a few of the tracked quantities provides more evidence of the propriety of the simulation results. Finally, the distinct trends observed between the mechanical energy produced by the major power producing muscles (VAS, GMAX, BFsh, and PSOAS) and pedaling rate lends further confidence in the model results.

With the propriety of the simulation results established, it is useful to discuss the results within the context of steady-state pedaling in the recumbent position. The VAS and GMAX muscles were the primary power generators in the extension region of the crank cycle whereas BFsh and PSOAS were the primary power generators in the flexion region of the crank cycle. The VAS, GMAX, BFsh, and PSOAS muscles worked as alternating pairs (Fig. 4) to generate power to the crank, as has been shown previously for both recumbent pedaling [22] and upright pedaling [9], [10], [40]. The triceps surae and TA muscles generated little power and functioned primarily to transfer power between the crank and limb segments. The triceps surae worked synergistically with the GMAX and VAS to deliver energy to the crank in the extension region of the crank cycle (Fig. 4), similar to upright pedaling [9], [10], [12]. In another synergistic relationship, TA transferred the power generated by PSOAS from the limb segments to the crank in the flexion region (Fig. 4).

The RF and HAM muscles functioned to transition the limb segments through the proximal and distal transition regions, respectively. RF delivered power to both the crank and limbs towards the end of the crank cycle. RF then delivered power to the crank and redistributed power from the limbs to the crank

through the rest of the proximal transition region (Fig. 4) to effect a smooth transition. The power generated and the power absorbed by the RF were low in other regions of the crank cycle. HAM delivered power to the crank in the distal transition region, as has been observed in simulations of upright pedaling [9], [10], [12]. However, HAM also absorbed power from the crank and transferred it to the limbs in the extension region (Fig. 4). As such, HAM acted as an energy sink and caused crank deceleration prior to accelerating the crank. HAM activity in the extension region is not atypical in recumbent pedaling, as it has been observed previously [22]. The function of the HAM in the extension region was to extend the hip prior to the distal transition because the intersegmental moment generated by the HAM at the hip is greater than that at the knee [9]. Similar to RF, HAM neither generated nor absorbed much power in the other regions of the crank cycle.

Pedaling rate affected the net mechanical energy generated by some of the muscles. The net mechanical energy decreased as pedaling rate increased in four (VAS, BFsh, PSOAS, and RF) of the nine muscle sets. The difference in the net mechanical energy from 40 to 60 rpm was most meaningful for three of the four primary power producing muscle sets namely VAS (8.3 J), BFsh (2.1 J), and PSOAS (4.5 J) (Table I). In contrast, the net mechanical energy generated by GMAX increased as pedaling rate increased (Table I). The GMAX power to the limbs also increased with pedaling rate (Fig. 5). One of the possible reasons for the observed trends is that the increased power of the GMAX helps compensate for the decreased power applied to the limbs by the VAS at the higher pedaling rates (Fig. 5). Another possibility is that the GMAX increased power to the limbs to overcome the higher viscous loads associated with the higher pedaling rates.

Comparisons of the changes in the percent of net mechanical energy contributions of the muscles provide insight into how the muscles adapt to the changes in pedaling rate. The percent of mechanical energy generated by six of the nine muscle sets exhibited either an increasing (BFsh, GMAX, and HAMS) or decreasing (VAS, PSOAS, and RF) trend with changes in pedaling rate (Table I). Of these six muscle sets, the VAS and GMAX contributions of mechanical energy were the most meaningful because they generated the highest percentage of the net mechanical energy for at least one pedaling rate and they had the greatest change in contribution across pedaling rates (16.1% change for VAS and 18.7% change for GMAX from 40 to 60 rpm) (Table I). As noted above, similar trends were observed for absolute contributions of net mechanical energy by these muscles.

An interesting result relates to the mechanical work performed by the BFsh and PSOAS muscles. The percent of the total mechanical work performed by the BFsh and PSOAS in this study (41% for the 50 rpm simulation) was larger than that in previous simulations of high pedaling rate and high workrate upright pedaling (about 16% in Raasch *et al.* [9] and about 26% in Neptune *et al.* [10]). However, the percent of total mechanical energy performed by the PSOAS in our simulations was within the range of values (10%–18%) reported previously for upright pedaling at higher pedaling rates and workrates [9], [10], [12], which indicates that the higher percent of the total mechanical work performed by the BFsh and PSOAS in

this study can be attributed to the BFsh. Additionally, the net mechanical energy generated by the BFsh in our study was similar to the values reported previously for 60 rpm upright pedaling at 120 W (about 7 J) [10] and at 264 W (about 10 J) [12]. These results suggest that the BFsh is preferentially recruited as part of a muscle recruitment hierarchy utilized to accomplish the pedaling task.

The results of this study provide new information on muscle coordination in recumbent pedaling that can be applicable to the development of pedaling therapies for rehabilitation within the range of pedaling rates tested in this study. For example, because the net and relative mechanical energy contributions of the primary power producing muscles (VAS, GMAX, BFsh, and PSOAS) are influenced by pedaling rate, the target pedaling rate could be set higher to decrease the net mechanical energy generated by VAS and thereby reduce the load on the ACL [6] and the patellofemoral contact forces [7]. Alternatively, if VAS training is the rehabilitation objective, then lower pedaling rates should be employed given that the absolute and relative contribution of the VAS decreased as pedaling rate increased. However, higher pedaling rates should be used if the objective is to increase the mechanical energy of the GMAX muscles. Because the GAS and SOL muscles generate little power, but instead contract largely isometrically to transfer power from the limb segments to the crank, low workrate recumbent pedaling exercises could be performed either by individuals with ankle musculotendon pathology (e.g., foot drop) using an ankle-foot orthosis or by individuals with ankle joint range-of-motion limitations.

There were some methodological issues associated with this study that deserve mention. First, the focus of this study was on pedaling rate dependent changes in muscle kinetics. While workrate dependent changes on muscle kinetics are another interesting issue, this was not examined in this study because we wanted to focus on a situation in which workrate may be the limiting factor, for example in pedaling by individuals with peripheral neuropathy or metabolic syndrome. The choice of 50 W was made because it is in the range of workrates that have been used in other therapeutic and rehabilitation studies (e.g., [1], [2], [38]).

Second, experimental data was collected from active cyclists wearing cleats. Active cyclists were used in the study because they were better able to maintain the target pedaling cadences. Because none of the study participants was a regular user of recumbent bicycles, their bicycling experience should not limit the applicability of the results of this study to a specific population. Cleats were used for practical reasons associated with defining a fixed point for the foot-pedal loads in the model necessary to calculate the intersegmental loads. The use of the cleats affects muscle forces for two reasons. One is that cleats enable muscles to generate crank torque in regions of the crank cycle other than the downstroke. As a result, the use of cleats leads to a decrease in the maximum crank torque [41] and VAS, HAM, and SOL muscular activity [42], [43] and an increase in the RF, BFsh, and TA muscular activity [42]. Accordingly, a rehabilitative pedaling exercise to reduce either the load on the ACL or patellofemoral contact forces should be performed at a higher pedaling rate and

with the foot fixed to the pedal. Moreover, cleats fix the anterior–posterior foot position on the pedal which influences the moment developed by the pedal reaction load about the ankle joint [44], [45] and the resulting forces developed by muscles, particularly the triceps surae [46]. Because cleats fix the anterior–posterior foot position, cleats should be used in rehabilitative pedaling exercises generally to develop consistent and predictable muscle forces and corresponding reaction loads on other musculoskeletal components.

In summary, this study completed a forward dynamic simulation to track steady-state low-power recumbent pedaling where muscle excitation timing from the simulation was consistent with that obtained experimentally and where the kinematic and kinetic quantities from the simulation tracked their experimental counterparts closely (i.e., generally within 1 SD). Analysis of the simulation results revealed that VAS, GMAX, PSOAS, and BFsh produce most of the power in low-power recumbent pedaling. The triceps surae muscles and TA function to transfer power from the limb segments to the crank and RF and HAM power the crank through the transition regions. Pedaling rate affects the power and hence energy produced by some of the muscles and the distribution of the energy, but the fundamental functions of the individual muscles do not change.

ACKNOWLEDGMENT

The authors would like to thank Prof. R. Neptune at the University of Texas, Austin for his assistance developing the model and providing the computer code to perform the muscle power analysis.

REFERENCES

- [1] K. L. Perell, R. J. Gregor, and A. M. E. Scremin, "Lower limb cycling mechanics in subjects with unilateral cerebrovascular accidents," *J. Appl. Biomechan.*, vol. 14, pp. 158–179, 1998.
- [2] K. L. Perell, S. Gregor, G. Kim, S. Rushatankov, A. M. E. Scremin, S. Levin, and R. Gregor, "Comparison of cycling kinetics during recumbent bicycling in subjects with and without diabetes," *J. Rehabil. Res. Develop.*, vol. 39, pp. 13–20, 2002.
- [3] P. D. Faghri, R. M. Glaser, and S. F. Figoni, "Functional electrical stimulation leg cycle ergometer exercise: Training effects on cardiorespiratory responses of spinal cord injured subjects at rest and during submaximal exercise," *Arch. Phys. Med. Rehabil.*, vol. 73, pp. 1085–1093, 1992.
- [4] S. P. Hooker, S. F. Figoni, M. M. Rodgers, R. M. Glaser, T. Mathews, A. G. Suryaprasad, and S. C. Gupta, "Physiologic effects of electrical stimulation leg cycle exercise training in spinal cord injured persons," *Arch. Phys. Med. Rehabil.*, vol. 73, pp. 470–476, 1992.
- [5] M. S. Nash, S. Bilsker, A. E. Marcillo, S. M. Isaac, L. A. Botelho, K. J. Klose, B. A. Green, M. T. Rountree, and J. D. Shea, "Reversal of adaptive left ventricular atrophy following electrically-stimulated exercise training in human tetraplegics," *Paraplegia*, vol. 29, pp. 590–599, 1991.
- [6] M. A. Hunt, D. J. Sanderson, H. Moffet, and J. T. Inglis, "Biomechanical changes elicited by an anterior cruciate ligament deficiency during steady rate cycling," *Clin. Biomechan.*, vol. 18, pp. 393–400, 2003.
- [7] E. Bressel, "The influence of ergometer pedaling direction on peak patellofemoral joint forces," *Clin. Biomechan.*, vol. 16, pp. 431–437, 2001.
- [8] B. J. Fregly and F. E. Zajac, "A state-space analysis of mechanical energy generation, absorption, and transfer during pedaling," *J. Biomechan.*, vol. 29, pp. 81–90, 1996.
- [9] C. C. Raasch, F. E. Zajac, B. Ma, and W. S. Levine, "Muscle coordination of maximum-speed pedaling," *J. Biomechan.*, vol. 30, pp. 595–602, 1997.

- [10] R. R. Neptune, S. A. Kautz, and F. E. Zajac, "Muscle contributions to specific biomechanical functions do not change in forward versus backward pedaling," *J. Biomechan.*, vol. 33, pp. 155–164, 2000.
- [11] R. R. Neptune and M. L. Hull, "A theoretical analysis of preferred pedaling rate selection in endurance cycling," *J. Biomechan.*, vol. 32, pp. 409–415, 1999.
- [12] F. E. Zajac, R. R. Neptune, and S. A. Kautz, "Biomechanics and muscle coordination of human walking—Part I: Introduction to concepts, power transfer, dynamics and simulations," *Gait Posture*, vol. 16, pp. 215–232, 2002.
- [13] B. R. Umberger, K. G. M. Gerritsen, and P. E. Martin, "Muscle fiber type effects on energetically optimal cadences in cycling," *J. Biomechan.*, vol. 39, pp. 1472–1479, 2006.
- [14] L. M. Schutte, M. M. Rodgers, F. E. Zajac, and R. M. Glaser, "Improving the efficacy of electrical stimulation-induced leg cycle ergometry: An analysis based on a dynamic musculoskeletal model," *IEEE Trans. Rehabil. Eng.*, vol. 1, no. 2, pp. 109–125, Jun. 1993.
- [15] M. Gfoehler and P. Lugner, "Dynamic simulation of FES-cycling: Influence of individual parameters," *IEEE Trans. Neural Syst. Rehabil. Eng.*, vol. 12, no. 4, pp. 398–405, Dec. 2004.
- [16] A. J. Van Soest, M. Gfoehler, and L. J. R. Casius, "Consequences of ankle joint fixation on FES cycling power output: A simulation study," *Med. Sci. Sports Exercise*, vol. 37, pp. 797–806, 2005.
- [17] B. R. MacIntosh, R. R. Neptune, and J. F. Horton, "Cadence, power, and muscle activation in cycle ergometry," *Med. Sci. Sports Exercise*, vol. 32, pp. 1281–1287, 2000.
- [18] A. P. Marsh and P. E. Martin, "The association between cycling experience and preferred and most economical cadences," *Med. Sci. Sports Exercise*, vol. 25, pp. 1269–1274, 1993.
- [19] A. P. Marsh and P. E. Martin, "The relationship between cadence and lower-extremity EMG in cyclists and noncyclists," *Med. Sci. Sports Exercise*, vol. 27, pp. 217–225, 1995.
- [20] G. Kohler and U. Boutellier, "The generalized force-velocity relationship explains why the preferred pedaling rate of cyclists exceeds the most efficient one," *Eur. J. Appl. Physiol.*, vol. 94, pp. 188–195, 2005.
- [21] R. R. Neptune, S. A. Kautz, and M. L. Hull, "The effect of pedaling rate on coordination in cycling," *J. Biomechan.*, vol. 30, pp. 1051–1058, 1997.
- [22] N. A. Hakansson and M. L. Hull, "Functional roles of the leg muscles when pedaling in the recumbent versus the upright position," *J. Biomechan. Eng.*, vol. 127, pp. 301–310, 2005.
- [23] R. R. Neptune and M. L. Hull, "Evaluation of performance criteria for simulation of submaximal steady-state cycling using a forward dynamic model," *J. Biomechan. Eng.*, vol. 120, pp. 334–341, 1998.
- [24] G. T. Yamaguchi and F. E. Zajac, "A planar model of the knee joint to characterize the knee extensor mechanism," *J. Biomechan.*, vol. 22, pp. 1–10, 1989.
- [25] S. L. Delp, J. P. Loan, M. G. Hoy, F. E. Zajac, E. L. Topp, and J. M. Rosen, "An interactive graphics-based model of the lower extremity to study orthopaedic surgical procedures," *IEEE Trans. Biomed. Eng.*, vol. 37, no. 8, pp. 757–767, Aug. 1990.
- [26] B. J. Fregly, F. E. Zajac, and C. A. Dairaghi, "Bicycle drive system dynamics: Theory and experimental validation," *J. Biomechan. Eng.*, vol. 122, pp. 446–452, 2000.
- [27] F. E. Zajac, "Muscle and tendon: Properties, models, scaling, and application to biomechanics and motor control," *Crit. Rev. Biomed. Eng.*, vol. 17, pp. 359–411, 1989.
- [28] M. J. Camilleri, M. L. Hull, and N. A. Hakansson, "Sloped muscle excitation waveforms improve the accuracy of forward dynamic simulations," *J. Biomechan.*, vol. 40, pp. 1423–1432, 2007.
- [29] M. G. Pandy, F. C. Anderson, and D. G. Hull, "A parameter optimization approach for the optimal control of large-scale musculoskeletal systems," *J. Biomechan. Eng.*, vol. 114, pp. 450–460, 1992.
- [30] W. L. Goffe, G. D. Ferrier, and J. Rogers, "Global optimization of statistical functions with simulated annealing," *Journal of Econometrics*, vol. 60, pp. 65–99, 1994.
- [31] R. D. Trumbower and P. D. Faghri, "Kinematic analyses of semi-reclined leg cycling in able-bodied and spinal cord injured individuals," *Spinal Cord*, vol. 43, pp. 543–549, 2005.
- [32] R. R. Neptune and M. L. Hull, "Accuracy assessment of methods for determining hip movement in seated cycling," *J. Biomechan.*, vol. 28, pp. 423–437, 1995.
- [33] J. Newmiller, M. L. Hull, and F. E. Zajac, "A mechanically decoupled two force component bicycle pedal dynamometer," *J. Biomechan.*, vol. 21, pp. 375–386, 1988.
- [34] E. F. Delagi, A. Perotto, J. Iazzetti, and D. Morrison, *Anatomic Guide for the Electromyographer—The Limbs*, 2nd ed. Springfield, IL: C. C. Thomas, 1974.
- [35] J. M. Winters and L. Stark, "Analysis of fundamental human movement patterns through the use of in-depth antagonistic muscle models," *IEEE Trans. Biomed. Eng.*, vol. 32, no. 10, pp. 826–839, Oct. 1985.
- [36] D. A. Brown, S. A. Kautz, and C. A. Dairaghi, "Muscle activity patterns altered during pedaling at different body orientations," *J. Biomechan.*, vol. 29, pp. 1349–1356, 1996.
- [37] D. A. Brown and S. A. Kautz, "Increased workload enhances force output during pedaling exercise in persons with poststroke hemiplegia," *Stroke*, vol. 29, pp. 598–606, 1998.
- [38] S. M. Gregor, K. L. Perell, S. Rushatankovik, E. Miyamoto, R. Muffoletto, and R. J. Gregor, "Lower extremity general muscle moment patterns in healthy individuals during recumbent cycling," *Clin. Biomechan.*, vol. 17, pp. 123–129, 2002.
- [39] P. W. Hodges and B. H. Bui, "A comparison of computer-based methods for the determination of onset of muscle contraction using electromyography," *Electroencephalogr. Clin. Neurophysiol.*, vol. 101, pp. 511–519, 1996.
- [40] L. H. Ting, S. A. Kautz, D. A. Brown, and F. E. Zajac, "Phase reversal of biomechanical functions and muscle activity in backward pedaling," *J. Neurophysiol.*, vol. 81, pp. 544–551, 1999.
- [41] R. R. Davis and M. L. Hull, "Measurement of pedal loading in bicycling: II. Analysis and results," *J. Biomechan.*, vol. 14, pp. 857–872, 1981.
- [42] M. O. Ericson, R. Nisell, U. P. Arborelius, and J. Ekholm, "Muscular activity during ergometer cycling," *Scand. J. Rehabil. Med.*, vol. 17, pp. 53–61, 1985.
- [43] M. Jorge and M. L. Hull, "Analysis of EMG measurements during bicycle pedaling," *J. Biomechan.*, vol. 19, pp. 683–694, 1986.
- [44] M. O. Ericson, J. Ekholm, O. Svensson, and R. Nisell, "The forces of ankle joint structures during ergometer cycling," *Foot Ankle*, vol. 6, pp. 135–142, 1985.
- [45] H. Gonzalez and M. L. Hull, "Multivariable optimization of cycling biomechanics," *J. Biomechan.*, vol. 22, pp. 1151–1161, 1989.
- [46] J. R. Van Sickle, Jr. and M. L. Hull, "Is economy of competitive cyclists affected by the anterior-posterior foot position on the pedal," *J. Biomechan.*, vol. 40, pp. 1262–1267, 2007.



Nils A. Hakansson received the B.A. degree in political science from Duke University in 1988. He attended San Francisco State University to fulfill the requirements of the Rehabilitation Engineering Technology Training Program from 1993 to 1995. He received the M.S. degree in biomedical engineering, in 2003, from the University of California, Davis, where he is currently working toward the Ph.D. degree also in biomedical engineering.

He taught English and worked as a copy editor in Beijing, China, from 1988 to 1991. His research interests include musculoskeletal biomechanics, neuromuscular control and coordination of human movement, and rehabilitation engineering applications.



M. L. Hull received the B.S. degree in mechanical engineering from Carnegie-Mellon University, in 1969, and the M.S. and Ph.D. degrees in mechanical engineering from the University of California, Berkeley, in 1970 and 1975, respectively.

Following a postdoctoral position in mechanical engineering at the University of California at Berkeley, he became a faculty member in the Mechanical Engineering Department at the University of California, Davis in 1976. In 1993, he became Chair of the Biomedical Engineering Graduate Program, a position which he held until 2000. His research activities encompass orthopedic biomechanics with emphasis on the human knee, musculoskeletal system modeling and simulation of movement, and sports biomechanics and equipment design particularly as related to cycling. His research contributions have been described in more than 155 papers published in scientific journals.